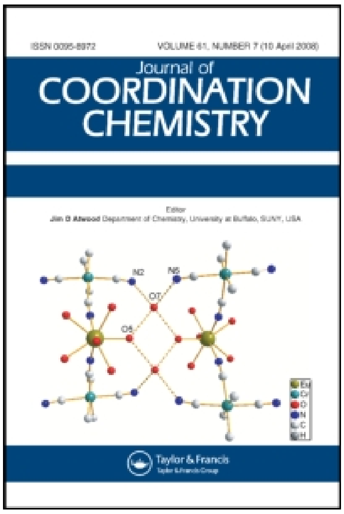

Journal of Coordination Chemistry

Publication details, including instructions for authors and subscription information:
http://www.informaworld.com/smpp/title~content=t713455674

Syntheses, crystal structures and magnetic properties of tungstato- and molybdo-bridged dinuclear copper(II) complexes

Mei-Ling Liu[a]; Wen Gu[a]; Zhen-Ping Ma[a]; Ping Zhu[a]; Yue-Qiang Gao[a]; Xin Liu[a]
[a] Department of Chemistry, Nankai University, Tianjin 300071, P.R. China

To cite this Article Liu, Mei-Ling , Gu, Wen , Ma, Zhen-Ping , Zhu, Ping , Gao, Yue-Qiang and Liu, Xin(2008) 'Syntheses, crystal structures and magnetic properties of tungstato- and molybdo-bridged dinuclear copper(II) complexes', Journal of Coordination Chemistry, 61: 21, 3476 — 3485

To link to this Article: DOI: 10.1080/00958970802068888

URL: http://dx.doi.org/10.1080/00958970802068888

Journal of Coordination Chemistry
Vol. 61, No. 21, 10 November 2008, 3476–3485

Taylor & Francis
Taylor & Francis Group

Syntheses, crystal structures and magnetic properties of tungstato- and molybdo-bridged dinuclear copper(II) complexes

MEI-LING LIU, WEN GU, ZHEN-PING MA, PING ZHU, YUE-QIANG GAO and XIN LIU*

Department of Chemistry, Nankai University, Weijin Road, Tianjin 300071, P.R. China

(*Received 4 December 2007; in final form 18 January 2008*)

Two new dinuclear copper(II) complexes, $[Cu_2(bpca)_2(WO_4)\ (H_2O)_2]\cdot H_2O$ (**1**) and $[Cu_2(bpca)_2(MoO_4)\ (H_2O)_2]\cdot H_2O$ (**2**) [bpca = *bis*(2-pyridylcarbonyl)amide anion], have been synthesized and their magnetic behavior investigated as a function of temperature. The structures of **1** and **2** have been determined by single-crystal X-ray diffraction. Complexes **1** and **2** are both 3D supramolecules with intermolecular hydrogen-bonding and π–π stacking interactions. The magnetic susceptibilities measured over the range 2–300 K show ferromagnetic interaction between the two copper(II) ions in **1**, while there is antiferromagnetic interaction between the two copper(II) ions in **2**. Based on the Hamiltonian written as $\hat{H} = -2JS_1 \cdot S_2$,best fitting for the experimental data leads to $J = 0.557\,\mathrm{cm}^{-1}$ (**1**) and $-77.2\,\mathrm{cm}^{-1}$ (**2**).

Keywords: Crystal structures; Magnetic properties; Copper complexes; Tungstate complex; Molybdate complex

1. Introduction

Bpca is a tridentate ligand through its three nitrogen atoms in mononuclear complexes $[M(bpca)_2]$, M = Mn(II) [1], Fe(II) [2], Cu(II) [3] and Zn(II) [3] and $[M(bpca)_2]X$ with M = Fe(III) ($X = ClO_4^-$) [2] and Rh(III) ($X = PF_6^-$) [4]. In these species, two mutually perpendicular bpca ligands build a distorted octahedral geometry around the metal ion. Each bpca in these complexes can additionally act as a bidentate ligand through its two carbonyl carbon atoms as revealed in the structures of $[M(bpca)_2\{M(hfa)_2\}]$ (M = Mn(II) and Fe(III); hfa = hexafluoroacetylacetone) [5] and $[Cu(bpca)]ClO_4$ [6].

The monoanionic character of bpca made isolation of neutral copper(II) species of formula Cu(bpca)X (X = monoanion) possible [7, 8–10]. Depending on the bridging ability of the X group, mononuclear ($X = NO_3^-$, NCS^- and CH_3COO^-) [7–9] or polynuclear compounds [$X = Cl^-$ and Br^-] [10] may result. In our research, we use $[Cu(bpca)]^+$ as a building block to design polynuclear copper(II) complexes with extended bridging ligands such as oxalate [11], squarate [12], croconate [13], 1,2- and 1,3-dithiosquarate [14] and 1,2-dithiocroconate [15]. Significant intramolecular

---

*Corresponding author. Email: liuxin64@nankai.edu.cn

Journal of Coordination Chemistry
ISSN 0095-8972 print/ISSN 1029-0389 online © 2008 Taylor & Francis
DOI: 10.1080/00958970802068888

copper(II)–copper(II) magnetic interactions (either ferro- or antiferromagnetic) have been observed.

As part of our magneto-structural studies with the paramagnetic $[Cu(bpca)]^+$ building block, we have prepared dinuclear copper(II) complexes $[Cu_2(bpca)_2(WO_4)(H_2O)_2] \cdot H_2O$ (**1**) and $[Cu_2(bpca)_2(MoO_4)(H_2O)_2 \cdot H_2O$ (**2**) [bpca = *bis*(2-pyridylcarbonyl) amide anion].

2. Results and discussion

2.1. *X-ray diffraction studies*

Both complexes are triclinic with metal ions interconnected by MO_4^{2-} (M = W, Mo) bridging two $[Cu(bpca)H_2O]^+$ units. Adjacent chains undergo π–π stacking forming a 2D architecture; in the crystal of both complexes an extensive hydrogen-bonding scheme gives a 3D supramolecular network.

Thermal ellipsoid drawing (30% probability) of **1** with the atomic numbering scheme is shown in figure 1. The structure consists of a dimeric unit with a symmetry axis, where both $[Cu(bpca)H_2O]^+$ cations are bridged by WO_4^{2-}. Each copper of the dinuclear entity is five-coordinate. A τ value of 0.23 indicates a distorted square pyramidal geometry. The copper(II) ions are linked to three N atoms of Hbpca [Cu(1)–N(1) = 1.987(4) Å, Cu(1)–N(2) = 1.936(4) Å and Cu(1)–N(3) = 2.007(4) Å] to the O(4) of WO_4^{2-}[Cu(1)–O(4) = 1.909(3) Å]. These four atoms (N1, N2, N3, O4) form the equatorial plane; the copper(II) ion deviates from this plane by 0.1009 Å. The apical position is occupied by one oxygen of a water [Cu(1)–O(3)= 2.370(4) Å]. The observed Cu–N and Cu–O distances are equivalent to similar complexes [16, 17]. The Cu(1)–O(3) distance is longer than the equatorial bond distances, partly because the fifth coordination position in square pyramidal arrangements is usually longer [18, 19]. Two $[Cu(bpca)H_2O]^+$ units are bridged by WO_4^{2-} to give a copper to copper separation of 5.5721(19) Å in the symmetric structure.

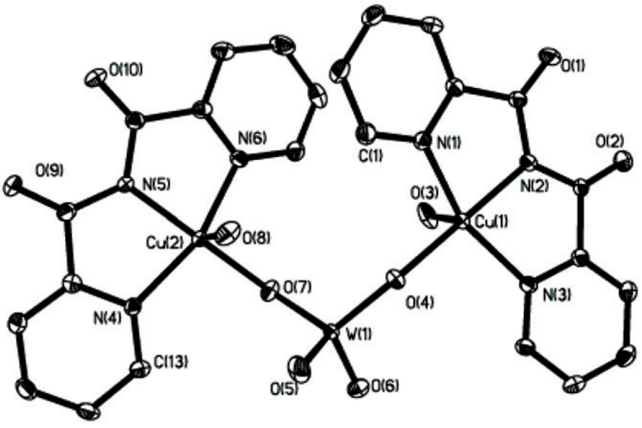

Figure 1. Molecular structure of **1** (hydrogen atoms and solvent moleculars are omitted for clarity).

π–π stacking and hydrogen-bonding give a 3D supramolecular network (figure 2). The shortest face-to-face distance (3.1634 Å) and dihedral angle (6.1°) between two bpca-rings of neighboring layer suggest the π–π interaction.

The copper in **2** is also five-coordinate (figure 3) with separation of adjacent coppers at 5.5497(9) Å. The crystal structure of **2** is similar to **1**. Figure 4 shows the 3D network of **2**. (The shortest face-to-face distance for π-stacking is 3.697 Å and the dihedral angle is 7.5°).

2.2. *Spectral properties*

The room temperature UV–Vis spectra of **1** in DMSO has a weak absorption band at 648 nm (figure 5), attributed to the *d–d* transition of Cu(II). UV-Vis spectra also give

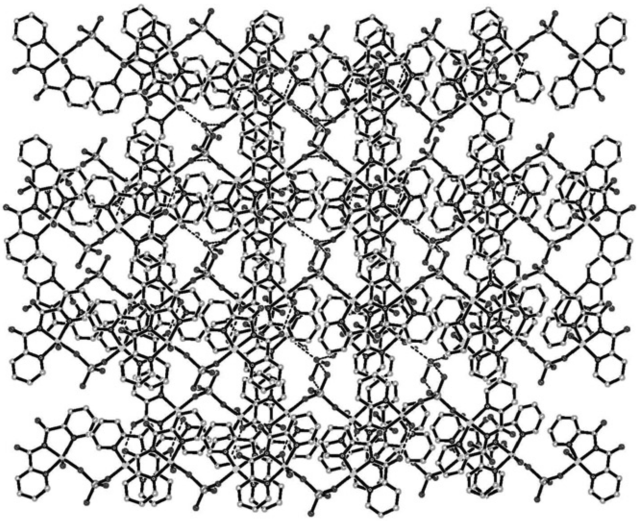

Figure 2. 3D network of **1**.

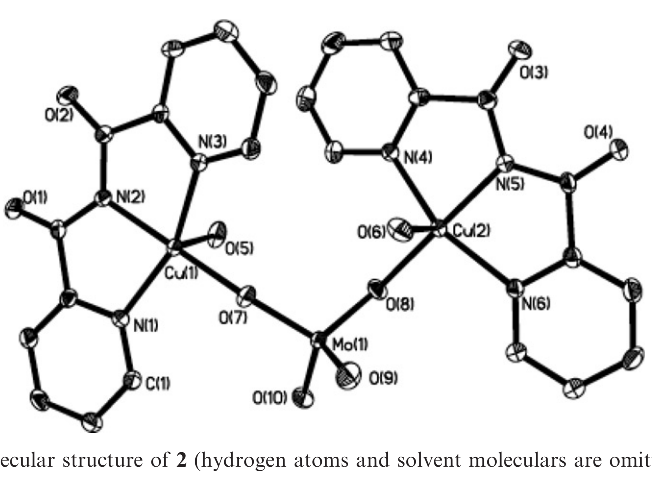

Figure 3. Molecular structure of **2** (hydrogen atoms and solvent moleculars are omitted for clarity).

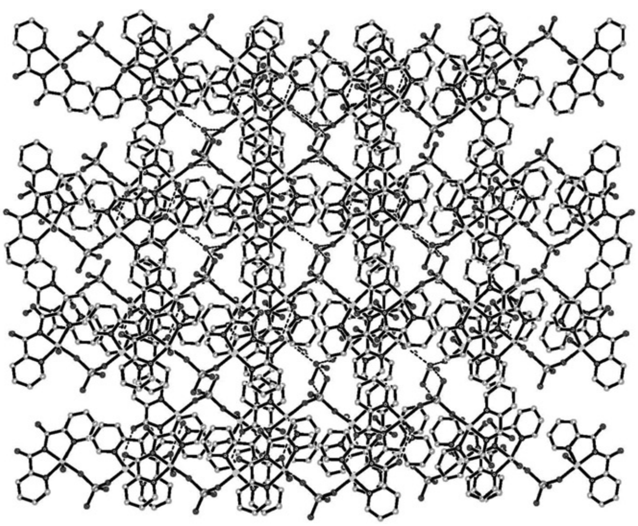

Figure 4. 3D network of **2**.

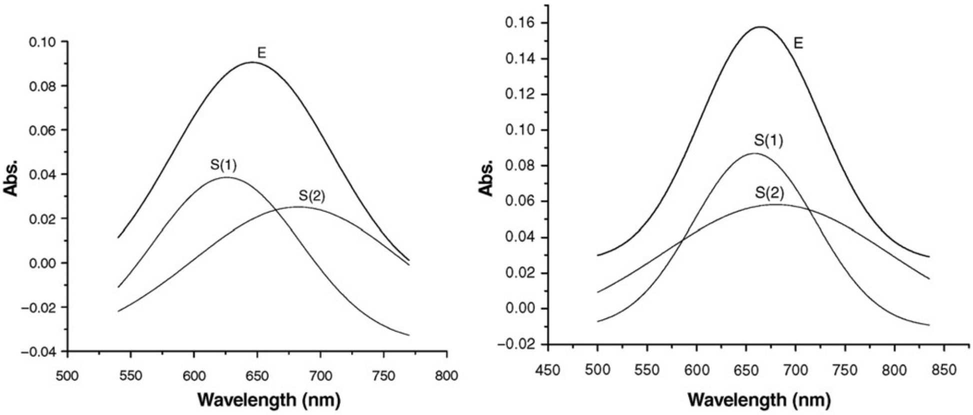

Complex **1**

Complex **2**

Figure 5. UV–Vis experimental spectrum (E) and Gauss stimulated spectrum (S) of **1** and **2**.

two weak bands (626, 682 nm) which on a tentatively square pyramidal geometry may correspond to the transitions: $^2B_1 \rightarrow {}^2B_2$, $^2B_1 \rightarrow {}^2A_1$. Comparably, **2** displays a weak absorption at 664 nm (figure 5), attributed to the *d–d* transition of Cu(II) from two bands (658, 680 nm) which on a tentatively square pyramidal geometry may correspond to the transitions: $^2B_1 \rightarrow {}^2E$, $^2B_1 \rightarrow {}^2B_2$.

2.3. *Magnetic properties*

Variable-temperature (2–300 K) magnetic susceptibility data at a magnetic field strength of 2 KG were collected for **1** (figure 6). The μ_{eff} at room temperature, 2.564 B.M., is slightly larger than the spin-only value of 2.449 B.M. for magnetically

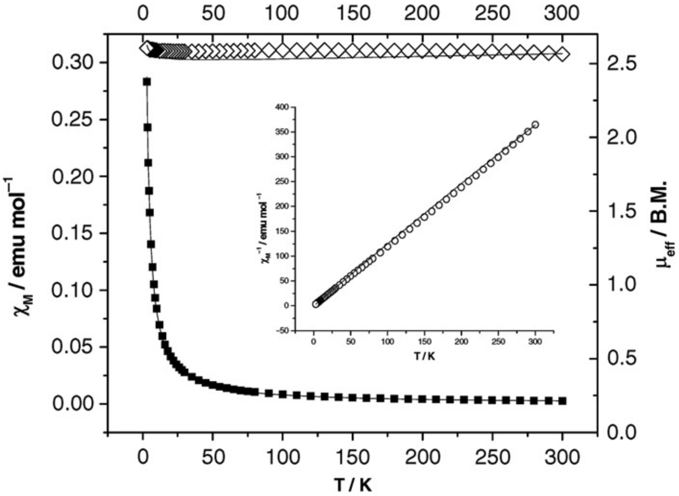

Figure 6. χ_M (■) *vs* T and μ_{eff} (□) *vs* T plots for **1**. The inset is the $1/\chi_M$ (○) *vs* T for **1**.

isolated single-spin Cu^{II}. When the temperature is lowed, the value of μ_{eff} increases, indicating that the spins are ferromagnetically coupled in **1**. From 100 K to 300 K, the data can be roughly fit to a Curie–Weiss law with $C = 0.832$ emu.K.mol^{-1} and $\theta = 0.308$ K. The Weiss constant is positive, which also indicates that the dominant magnetic interaction is ferromagnetic. The Hamiltonian for **1** can be written [20, 21]:

$$\chi_M = \frac{2Ng^2\beta^2}{k(T-\theta)}[3+\exp(-2J/kT)]^{-1}(1-\rho)+\frac{Ng^2\beta^2}{2kT}+N\alpha$$

Best fitting for the experimental data leads to $J = 0.557\,\mathrm{cm}^{-1}$, $g = 2.049$ with the agreement factor $R = \sum(\chi_{obsd} - \chi_{cacld})^2/\chi^2_{obsd} = 6.4 \times 10^{-4}$. Compared with the reported dinuclear Cu(II) complex $[Cu_2(bpca)_2(H_2O)_2(C_2O_4)] \cdot 2H_2O$ (Cu–Cu separation of 7.460(1) Å, $J = 1.1\,\mathrm{cm}^{-1}$) [22], **1** displays weaker ferromagnetic properties (Cu–Cu separation of 5.5721(19) Å).

Variable-temperature (2–300 K) magnetic susceptibility data at a magnetic field strength of 2 KG were collected for **2** (figure 7). The μ_{eff} at room temperature, 2.54 B.M., is slightly larger than the spin-only value of 2.449 B.M. for magnetically isolated single-spin Cu^{II}. When the temperature is lowed, the value of μ_{eff} decreases, indicating that the spins are antiferromagnetically coupled. From 100 K to 300 K, the data can be roughly fit to a Curie–Weiss law with $C = 1.0979$ emu. K. mol^{-1} and $\theta = -113.09$ K. The Weiss constant is negative, which also indicates that the dominant magnetic interaction is antiferromagnetic. The Hamiltonian for **2** can be written [20, 21]:

$$\chi_M = \frac{2Ng^2\beta^2}{k(T-\theta)}[3+\exp(-2J/kT)]^{-1}(1-\rho)+\frac{Ng^2\beta^2}{2kT}+N\alpha$$

Best fitting for the experimental data leads to $J = -77.2\,\mathrm{cm}^{-1}$, $g = 2.06$ with the agreement factor $R = \sum\,(\chi_{obsd} - \chi_{cacld})^2/\chi^2{}_{obsd} = 3.18 \times 10^{-4}$. Compared with the reported

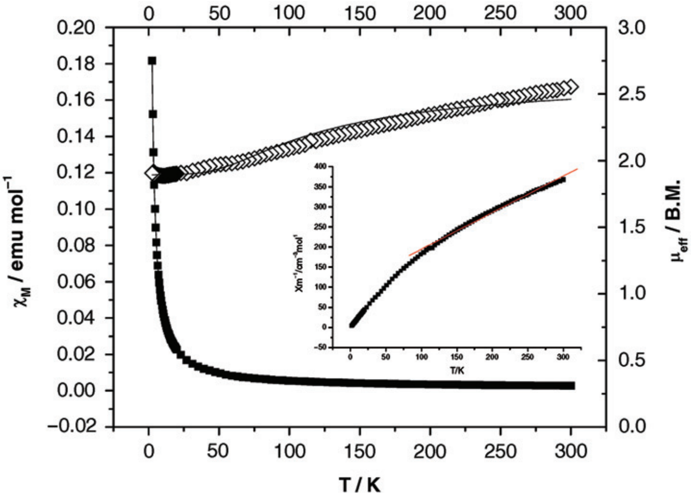

Figure 7. χ_M (■) *vs*. T and μ_{eff} (□) *vs* T plots for **2**. The inset is the $1/\chi_M$ (○) *vs* T for **2**.

Table 1. Crystal data and structure refinement for **1** and **2**.

Empirical formula	$C_{24}H_{22}Cu_2N_6O_{11}W$ (**1**)	$C_{24}H_{22}Cu_2N_6O_{11}Mo$ (**2**)
Formula weight	881.41	793.50
Temperature (K)	294(2)	293(2)
λ (Mo-*Kα*)(Å)	0.71073	0.71073
Crystal system	Triclinic	Triclinic
Space group	$P\bar{1}$	$P\bar{1}$
Unit cell dimensions (Å, °)		
a	10.263(3)	10.2788(10)
b	10.453(3)	10.4523(10)
c	13.559(5)	13.5621(14)
α	77.098(6)	77.3250(10)
β	69.845(5)	69.7020(10)
γ	85.096(5)	85.1780(10)
V (Å^3)	1331.0(8)	1333.2(2)
Z	2	2
D_{Calcd} (Mg m^{-3})	2.199	1.977
Abs. coeff. (mm^{-1})	5.969	2.119
F (000)	856	792
Crystal size (mm^3)	0.22 × 0.16 × 0.12	0.28 × 0.22 × 0.14
2θ range (°)	1.64–26.29	2.00 to 25.03
Reflections collected	7465	7251
Unique reflections	5259 [R(int) = 0.0230]	4650 [R(int) = 0.0202]
Absorption correction	Semi-empirical from equivalents	Semi-empirical from equivalents
Max. and min. transmission	1.000000 and 0.576970	1.000000 and 0.417418
Refinement method	Full-matrix least-squares on F^2	Full-matrix least-squares on F^2
Data/restraints/parameters	5259/9/421	4650/0/398
Goodness-of-fit on F^2	1.001	1.058
Final R indices [$I > 2\sigma(I)$]	$R_1 = 0.0300$, $wR_2 = 0.0651$	$R_1 = 0.0332$, $wR_2 = 0.0743$
R indices (all data)	$R_1 = 0.0392$, $wR_2 = 0.0691$	$R_1 = 0.0524$, $wR_2 = 0.0828$
Largest diff. peak hole (e Å^{-3})	1.293 and −1.460	0.428 and −0.569

Table 2. Selected bond lengths [Å] and angles [°] for **1**.

W(1)–O(6)	1.735(3)	Cu(1)–N(3)	2.007(4)
W(1)–O(5)	1.736(3)	Cu(1)–O(3)	2.370(4)
W(1)–O(4)	1.781(3)	Cu(2)–O(7)	1.925(3)
W(1)–O(7)	1.818(3)	Cu(2)–N(5)	1.936(4)
Cu(1)–O(4)	1.909(3)	Cu(2)–N(6)	1.992(4)
Cu(1)–N(2)	1.936(4)	Cu(2)–N(4)	2.013(4)
Cu(1)–N(1)	1.987(4)	Cu(2)–O(8)	2.324(4)
O(6)–W(1)–O(5)	109.32(18)	N(5)–Cu(2)–O(8)	94.81(15)
O(6)–W(1)–O(4)	110.04(17)	N(6)–Cu(2)–O(8)	95.49(16)
O(5)–W(1)–O(4)	109.10(18)	N(4)–Cu(2)–O(8)	96.33(15)
O(6)–W(1)–O(7)	106.86(17)	Cu(1)–O(3)–H(3A)	136(3)
O(5)–W(1)–O(7)	109.80(17)	Cu(1)–O(3)–H(3B)	108(3)
O(4)–W(1)–O(7)	111.68(16)	W(1)–O(4)–Cu(1)	154.5(2)
O(4)–Cu(1)–N(2)	177.25(17)	W(1)–O(7)–Cu(2)	134.1(2)
O(4)–Cu(1)–N(1)	96.99(15)	Cu(2)–O(8)–H(8A)	112(4)
N(2)–Cu(1)–N(1)	81.76(16)	Cu(2)–O(8)–H(8B)	114(4)
O(4)–Cu(1)–N(3)	98.29(15)	C(1)–N(1)–Cu(1)	127.7(3)
N(2)–Cu(1)–N(3)	82.33(16)	C(5)–N(1)–Cu(1)	113.4(3)
N(1)–Cu(1)–N(3)	159.14(17)	C(6)–N(2)–Cu(1)	117.7(3)
O(4)–Cu(1)–O(3)	94.46(15)	C(7)–N(2)–Cu(1)	117.4(3)
N(2)–Cu(1)–O(3)	88.18(16)	C(12)–N(3)–Cu(1)	128.0(3)
N(1)–Cu(1)–O(3)	100.68(16)	C(8)–N(3)–Cu(1)	112.7(3)
N(3)–Cu(1)–O(3)	92.21(16)	C(13)–N(4)–Cu(2)	128.6(3)
O(7)–Cu(2)–N(5)	174.13(16)	C(17)–N(4)–Cu(2)	112.6(3)
O(7)–Cu(2)–N(6)	97.37(16)	C(18)–N(5)–C(19)	124.3(4)
N(5)–Cu(2)–N(6)	81.28(16)	C(18)–N(5)–Cu(2)	117.9(3)
O(7)–Cu(2)–N(4)	98.28(15)	C(19)–N(5)–Cu(2)	117.8(3)
N(5)–Cu(2)–N(4)	81.91(16)	C(20)–N(6)–C(24)	118.8(4)
N(6)–Cu(2)–N(4)	160.17(16)	C(20)–N(6)–Cu(2)	113.7(3)
O(7)–Cu(2)–O(8)	91.00(14)	C(24)–N(6)–Cu(2)	127.5(3)

dinuclear Cu(II) complex [{Cu(acpa)}$_2$(μ-MoO$_4$)] $\cdot$ 4H$_2$O (Cu–Cu separation of 6.703(2) Å, $2J = -5.1(4)\,\mathrm{cm}^{-1}$) [23], **2** displays antiferromagnetic properties (Cu–Cu separation of 5.5497(9) Å).

3. Experimental

3.1. *Physical measurements*

Infrared spectra as KBr pellets were recorded on a Bruker Tensor 27 spectrophotometer in the range 4000–400 cm^{-1}. UV–Vis spectra in DMSO were recorded on a Jasco V-570 UV–Vis scanning spectrophotometer.

3.2. *Starting materials*

Na$_2$MoO$_4$ and Na$_2$WO$_4$ were of analytical grade obtained from commercial sources and used without further purification. [Cu(bpca) (H$_2$O)$_2$(O$_2$CCH$_3$)] $\cdot$ H$_2$O was synthesized according to the literature [24].

Table 3. Selected bond lengths [Å] and angles [°] for **2**.

Cu(1)–O(7)	1.910(3)	Cu(2)–N(4)	1.999(3)
Cu(1)–N(2)	1.934(3)	Cu(2)–N(6)	2.023(3)
Cu(1)–N(3)	1.992(3)	Cu(2)–O(6)	2.322(3)
Cu(1)–N(1)	2.010(3)	Mo(1)–O(9)	1.714(3)
Cu(1)–O(5)	2.374(3)	Mo(1)–O(10)	1.724(3)
Cu(2)–O(8)	1.919(3)	Mo(1)–O(7)	1.772(3)
Cu(2)–N(5)	1.938(3)	Mo(1)–O(8)	1.808(3)
O(7)–Cu(1)–N(2)	177.31(14)	O(9)–Mo(1)–O(8)	109.83(14)
O(7)–Cu(1)–N(3)	96.87(13)	O(10)–Mo(1)–O(8)	107.36(14)
N(2)–Cu(1)–N(3)	81.76(13)	O(7)–Mo(1)–O(8)	111.34(13)
O(7)–Cu(1)–N(1)	98.34(12)	Cu(1)–O(5)–H(5A)	139.3
N(2)–Cu(1)–N(1)	82.45(13)	Cu(1)–O(5)–H(5B)	104.4
N(3)–Cu(1)–N(1)	159.59(13)	Cu(2)–O(6)–H(6A)	112.1
O(7)–Cu(1)–O(5)	94.25(11)	Cu(2)–O(6)–H(6B)	108.5
N(2)–Cu(1)–O(5)	88.28(12)	Mo(1)–O(7)–Cu(1)	154.33(18)
N(3)–Cu(1)–O(5)	100.66(12)	Mo(1)–O(8)–Cu(2)	134.25(16)
N(1)–Cu(1)–O(5)	91.71(12)	C(1)–N(1)–Cu(1)	128.2(3)
O(8)–Cu(2)–N(5)	174.08(13)	C(5)–N(1)–Cu(1)	112.5(3)
O(8)–Cu(2)–N(4)	97.59(13)	C(7)–N(2)–Cu(1)	117.9(3)
N(5)–Cu(2)–N(4)	81.19(13)	C(6)–N(2)–Cu(1)	117.1(3)
O(8)–Cu(2)–N(6)	98.38(13)	C(12)–N(3)–Cu(1)	127.7(3)
N(5)–Cu(2)–N(6)	81.67(13)	C(8)–N(3)–Cu(1)	113.6(3)
N(4)–Cu(2)–N(6)	159.96(13)	C(17)–N(4)–Cu(2)	113.9(3)
O(8)–Cu(2)–O(6)	91.45(11)	C(13)–N(4)–Cu(2)	127.1(3)
N(5)–Cu(2)–O(6)	94.43(12)	C(19)–N(5)–Cu(2)	118.3(3)
N(4)–Cu(2)–O(6)	95.70(12)	C(18)–N(5)–Cu(2)	117.7(3)
N(6)–Cu(2)–O(6)	95.90(12)	C(24)–N(6)–C(20)	118.8(3)
O(9)–Mo(1)–O(10)	109.41(15)	C(24)–N(6)–Cu(2)	128.2(3)
O(9)–Mo(1)–O(7)	109.23(15)	C(20)–N(6)–Cu(2)	113.0(3)
O(10)–Mo(1)–O(7)	109.63(14)		

3.3. *Preparations of compounds*

3.3.1. [Cu$_2$(bpca)$_2$(WO$_4$) (H$_2$O)$_2$] · H$_2$O (1). Na$_2$WO$_4$ (0.5 mmol) was dissolved in water (7 mL) and a solution of [Cu(bpca) (H$_2$O)$_2$(O$_2$CCH$_3$)] · H$_2$O (0.5 mmol) in ethanol (8 mL) was added. The solution was stirred for 1 h and the light blue precipitatate was filtered off. The filtrate was kept for three weeks at ambient conditions, and blue, block crystals of **1** were isolated in 42% yield (based on copper). Elemental analysis (%) Calcd for C$_{24}$H$_{22}$Cu$_2$N$_6$O$_{11}$W: C, 41.48; H, 3.19; N, 11.89. Found: C, 41.33; H, 3.12; N, 12.05. IR (KBr pellet): 3454(s), 1716(s), 831(s).

3.3.2. [Cu$_2$(bpca)$_2$(MoO$_4$) (H$_2$O)$_2$] · H$_2$O (2). [Cu(bpca) (H$_2$O)$_2$(O$_2$CCH$_3$)] · H$_2$O (0.5 mmol) and Na$_2$MoO$_4$ (0.2 mmol) were dissolved in water/methanol (1/1 V/V, 12 mL). The resulting blue solution was placed in a 25-mL teflon-lined autoclave and heated at 413 K for 4 h and then cooled to room temperature over 5 h. The resulting blue cubic crystals obtained from the solution by pipette were washed with methanol and water. The yield is approximately 55% (based on Cu). Elemental analysis (%) calcd for C$_{24}$H$_{22}$Cu$_2$N$_6$O$_{11}$Mo: C, 41.61; H, 3.11; N, 12.01. Found: C, 41.50; H, 3.18; N, 12.05. IR (KBr pellet): 3442(s), 1706(s), 861(s).

3.4. *X-ray structure analysis*

Structural measurements of the two complexes were performed on a computer controlled Bruker SMART 1000 CCD diffractometer equipped with graphite-monochromated Mo-$K\alpha$ radiation with radiation wavelength 0.71073 Å at room temperature by using the ω-scan technique. Lorentz polarization and absorption corrections were applied. The structures were solved using SHELXL-97 and refined by the full-matrix least-squares method. Non-hydrogen atoms were refined anisotropically. Hydrogen atoms were located from the difference Fourier map and refined. Crystal data and structure refinement for **1** and **2** are shown in table 1, and selected bond lengths and angles for **1** and **2** are given in tables 2 and 3.

Supplementary material

Crystallographic data (excluding structure factors) for the structures in this article have been deposited with Cambridge Crystallographic Data Centre as supplementary publication CCDC Nos. 289128 and 602390. Copies of the data can be obtained free of charge on application to Cambridge Crystallographic Data Centre, 12 Union Road, Cambridge CB2 1EZ, UK (Fax: -44-1223-336033; E-mail for inquiry: fileserv@ ccdc.cam.ac.uk; V-email for deposition: deposit@ccdc.cam.ac.uk).

Acknowledgements

This work was supported by the National Natural Science Foundation of China (Grants 20371027 and 20071020) and the Tianjin Science Foundation (Grant 033609211).

References

[1] D. Marcos, J.V. Folgado, D. Beltrán-Porter, M.T. Do Prado Gambardella, S.H. Pulcinelli, R.H. De Almeida-Santos. *Polyhedron*, **9**, 2699 (1990).

[2] S. Wocadlo, W. Massa, J.V. Folgado. *Inorg. Chim. Acta*, **207**, 199 (1993).

[3] D. Marcos, R. Martinez-Manez, J.V. Folgado, A. Beltrán-Porter, D. Beltrán-Porter, A. Fuertes. *Inorg. Chim. Acta*, **159**, 11 (1989).

[4] P. Paul, B. Tyagi, M.M. Bhadbhade, E. Suresh. *J. Chem. Soc., Dalton Trans.*, 2273 (1997).

[5] T. Kajiwara, T. Ito. *J. Chem. Soc., Dalton Trans.*, 3351 (1998).

[6] A. Cantarero, J.M. Amigo, J. Faus, M. Julve, T. Debaerdemaeker. *J. Chem. Soc., Dalton Trans.*, 2033 (1988).

[7] I. Castro, J. Faus, M. Julve, J.M. Amigo, J. Sletten, T. Debaerdemaeker. *J. Chem. Soc., Dalton Trans.*, 891 (1990).

[8] J.V. Folgado, E. Martinez-Tamayo, A. Beltrán-Porter, D. Beltrán-Porter. *Polyhedron*, **8**, 1077 (1989).

[9] G. Madariaga, F.J. Zuniga, T. Rojo, J.V. Folgado. *Acta Crystallogr., Sect C*, **47**, 1632 (1991).

[10] J.V. Folgado, E. Coronado, D. Beltrán-Porter, R. Burriel, A. Fuertes, C. Miravitlles. *J. Chem. Soc., Dalton Trans.*, 3041 (1988).

[11] I. Castro, J. Faus, M. Julve, M. Mollar, A. Monge, E. Gutierrez-Puebla. *Inorg. Chim. Acta*, **161**, 97 (1989).

[12] I. Castro, J. Faus, M. Julve, Y. Journaux, J. Sletten. *J. Chem. Soc., Dalton Trans.*, 2533 (1991).

[13] I. Castro, J. Sletten, J. Faus, M. Julve, Y. Journaux, F. Lloret, S. Alvarez. *Inorg. Chem.*, **31**, 1889 (1992).
[14] I. Castro, M.L. Calatayud, J. Sletten, F. Lloret, J. Cano, M. Julve, G. Seitz, K. Mann. *Inorg. Chem.*, **38**, 4680 (1999).
[15] J. Sletten, M. Julve, F. Lloret, I. Castro, G. Seitz, K. Mann. *Inorg. Chim. Acta*, **250**, 219 (1996).
[16] G.T. Musie, X.B. Li, D.R. Powell. *Inorg. Chim. Acta*, **348**, 69 (2003).
[17] A. Neves, C.N. Verni, M.A. de Brito, I. Vencato, A. Mangrich, G. Oliva, D.D.H.F. Souza, A.A. Batista. *Inorg. Chim. Acta*, **290**, 207 (1999).
[18] I. Murase, G. Vuckovic, M. Kodera, H. Harada, N. Matsumoto, S. Kida. *Inorg. Chem.*, **30**, 728 (1991).
[19] N.A. Bailey, D.E. Fenton, M.V. Franklin, M. Hall. *J. Chem. Soc., Dalton Trans.*, 984 (1980).
[20] K. Sanjib, C. Nripen, D. Anindya. *Inorg. Chem.*, **43**, 4911 (2004).
[21] G. Sandeep, S. Biprajit, P. Srikanta. *J. Chem. Soc., Dalton Trans.*, 706 (2005).
[22] M.L. Calatayud, I. Castro, J. Sletten, F. Lloret, M. Julve. *Inorg Chim. Acta*, **300–302**, 846 (2000).
[23] H. Oshio, T. Kikuchi, T. Ito. *Inorg. Chem.*, **35**, 4938 (1996).
[24] J.V. Folgado, E. Martinez-Tamayo, A. Beltrán-Porter, D. Beltrán-Porter, A. Fuertes, C. Miravitlles. *Polyhedron*, **8**, 1077 (1989).